Physical Chemistry in Action

Steen Brøndsted Nielsen
Jean Ann Wyer *Editors*

Photophysics of Ionic Biochromophores

Springer

Physical Chemistry in Action

For further volumes:
http://www.springer.com/series/10915

Steen Brøndsted Nielsen • Jean Ann Wyer
Editors

Photophysics of Ionic Biochromophores

Springer

Editors
Steen Brøndsted Nielsen
Jean Ann Wyer
Faculty of Science and Technology
Department of Physics and Astronomy
Aarhus University
Aarhus
Denmark

ISSN 2197-4349 ISSN 2197-4357 (electronic)
ISBN 978-3-642-40189-3 ISBN 978-3-642-40190-9 (eBook)
DOI 10.1007/978-3-642-40190-9
Springer Heidelberg New York Dordrecht London

Library of Congress Control Number: 2013950272

© Springer-Verlag Berlin Heidelberg 2013
This work is subject to copyright. All rights are reserved by the Publisher, whether the whole or part of the material is concerned, specifically the rights of translation, reprinting, reuse of illustrations, recitation, broadcasting, reproduction on microfilms or in any other physical way, and transmission or information storage and retrieval, electronic adaptation, computer software, or by similar or dissimilar methodology now known or hereafter developed. Exempted from this legal reservation are brief excerpts in connection with reviews or scholarly analysis or material supplied specifically for the purpose of being entered and executed on a computer system, for exclusive use by the purchaser of the work. Duplication of this publication or parts thereof is permitted only under the provisions of the Copyright Law of the Publisher's location, in its current version, and permission for use must always be obtained from Springer. Permissions for use may be obtained through RightsLink at the Copyright Clearance Center. Violations are liable to prosecution under the respective Copyright Law.
The use of general descriptive names, registered names, trademarks, service marks, etc. in this publication does not imply, even in the absence of a specific statement, that such names are exempt from the relevant protective laws and regulations and therefore free for general use.
While the advice and information in this book are believed to be true and accurate at the date of publication, neither the authors nor the editors nor the publisher can accept any legal responsibility for any errors or omissions that may be made. The publisher makes no warranty, express or implied, with respect to the material contained herein.

Printed on acid-free paper

Springer is part of Springer Science+Business Media (www.springer.com)

Preface

Spectroscopy of isolated biomolecular ions *in vacuo* has within the last decade or so become a highly active research field, both for experimentalists and theorists, made possible by the development of advanced instrumental apparatus and the steady increase in more powerful computers. The field is highly interdisciplinary including researchers in chemistry, physics, and molecular biology. Absorption spectra of isolated ions shed light on the intrinsic electronic structures without perturbations from say water molecules, counter ions, nearby charges, or polar amino acids. A comparison with spectra of the chromophores in their natural environment then allows one to identify possible perturbations. Spectra at the same time provide important benchmarks for quantum chemical calculations of electronically excited states, which is still a non-trivial task. Not only absorption spectra but also fluorescence spectra are excellent indicators of environmental effects. In this volume, we focus on spectroscopy of protein chromophores, amino acids and peptides, to whole proteins and DNA nucleotides and oligonucleotides. Dissociation channels and timescales for deexcitation and dissociation are also discussed in detail, as they shed important light on energy-flow processes within the isolated biomolecular ion; indeed, small molecular ions with few degrees of freedom are destined to break apart after photoexcitation due to the absence of a heat bath (energy sink). As all systems included here are ionic, mass spectrometry in combination with lasers are used for the experiments. Experimental techniques to measure spectra and theoretical methods commonly employed are described with a discussion on limitations and advantages.

Our book comprises 11 chapters each written by one or more experts in the topic. The book is organised as follows: At the beginning of the book, even before the General Introduction, there are explanatory pages (Concepts) for non-experts in the field where we briefly describe electric- and magnetic-field sectors used as ion deflectors, photophysical processes illustrated by Jablonski diagrams, molecular orbital theory, solvatochromic shifts of electronic transitions, peptide and nucleic acids structures, and nomenclature regarding peptide fragmentation. Our hope is that with these sections, the book shows potential to be used for graduate teaching courses in photobiology and not just for researchers within the field. The second chapter is a brief introduction by one of us (Brøndsted Nielsen) discussing

biochromophore ions and the role of microenvironments such as water or nearby charge sites. The chapter ends by touching upon possible future directions for the field. In the next chapter, Wyer introduces the experimental techniques used for performing gas-phase spectroscopy of ions with emphasis on ion storage rings and other home-built ion beam set-ups as these are less well described in the literature. It is certainly true that no experiment is perfect, and Wyer discusses the advantages and disadvantages with different set-ups, differences between positive and negative ions and importantly what to be cautious about when interpreting experimental results. In the next chapter by Rubio and Wanko, theoretical methods that are commonly employed to describe these rather big systems are presented. Also here the methods are carefully evaluated and their performances relative to each other are discussed. The subsequent chapters deal with actual biochromophores and their photophysics. The chapter by Andersen and Bochenkova gives an overview of the GFP chromophore anion and its absorption spectrum; this spectrum from 2001 was the first to be obtained for an isolated biochromophore ion. The authors discuss the competition between electron photodetachment and internal conversion, which is an issue that needs to be considered for anions whose detachment energies are within the absorption band. The next chapter by Brøndsted Nielsen deals with the detection of light emitted from photoexcited chromophore ions (dyes), which is even harder experimentally than obtaining an absorption spectrum. Still fluorescence spectroscopy has proven to be a very strong tool for monitoring structures of isolated biomolecular ions. Wyer and Brøndsted Nielsen summarise in the following chapter the increasing amount of data on porphyrin and heme ions and their complexes with amino acids and NO and compare results with protein spectra. Also two-laser experiments are discussed allowing one to record spectra of long-lived photoexcited ions. Spectra of whole proteins are presented in the next chapter by Antoine and Dugourd, where either heme or aromatic amino acid residues are the absorbing species. The authors demonstrate the importance of the charge state in obtaining action spectra, and from two-laser experiments they nicely succeed in performing spectroscopy on radical species. Dedonder, Féraud, and Jouvet provide a comprehensive review of the field of spectroscopy of protonated amino acids and small peptide ions, both at room temperature and at low temperature, with emphasis on the fast dissociation channels that are operative when the ions are electronically excited and that compete with internal conversion to the electronic ground state; their relative importance is measured from photodissociation of the ions in an electric field. The number of fragments formed in a dissociation process is found from coincidence experiments considering momentum conservation. Timescales for the deexcitation processes are established from femtosecond pump-probe laser experiments. Their work nicely demonstrates how experimental results and theoretical ones go hand in hand in obtaining the deepest level of understanding. DNA and RNA nucleotides and oligonucleotides are the focus of the chapter by Weber, Marcum, and Brøndsted Nielsen who in detail discuss UV-induced fragmentation channels, timescales for dissociation after photoexcitation and whether dissociation is statistical or nonstatistical, and finally electronic spectra (both absorption and photoelectron spectra). In this chapter the complex role of multiple light absorbing

species is also considered. In all of these works either visible or UV light was used for the experiments. In the final chapter by Schlathölter and Hoekstra, recent work in extending the wavelength region to the vacuum ultraviolet is presented, and the importance of this region is clearly emphasised by work on peptide ions.

Let us end by saying that the chosen topics for this volume present a selection of important scientific contributions that *we* believe have been made to this rapidly increasing field. They are of course biased by our own interests, and other important work could have been covered, *e.g.* the electronic properties of simpler molecular ions isolated *in vacuo* that were earlier explored. However, we hope that the reader has got an impression after reading all the chapters of the rich possibilities that exist to form and study complicated and fragile ions *in vacuo*, and that, most importantly, new fundamental science is learned from such work. We would like to take the opportunity to thank all the authors who have contributed to this volume and in our opinion have made this volume a most timely one and one of very high quality.

Aarhus, June 25, 2013 Steen Brøndsted Nielsen and Jean Ann Wyer

Abbreviations

A	Acceptor
	Adenine
ADE	Adiabatic Detachment Energy
AI	Auto Ionising
AMP	Adenosine MonoPhosphate
ATP	Adenosine TriPhosphate
BBO	Barium BOrate
BIRD	Blackbody Infrared Radiative Dissociation
C	Cytosine
CA	Connection-Atom
CAD	Collisional Activated Dissociation (high energy, $>$ keV)
CAM	Coulomb-Attenuation Method
CASSCF	Complete Active Space Self-Consistent Field
CC	Coupled Cluster
CE	Crown Ether
CI	Conical Intersection
CID	Collision Induced Dissociation (low energy, $<$100 eV)
CIS	Configuration Interaction Singles
CPE	Chemical Potential Equilibration
CT	Charge Transfer
CW	Continuous Wave
D	Donor
	Dye
DDCI	Difference-Dedicated Conical Intersection
DFT	Density Functional Theory
DMSO	DiMethylSulfOxide
DNA	DeoxyriboNucleic Acid
EA	Electron Affinity
EBE	Electron Binding Energy
ECD	Electron Capture Dissociation
EDD	Electron Detachment Dissociation

EGP	Effective Group Potential
ELISA	ELectrostatic Ion Storage ring in Aarhus
EOM	Equation-Of-Motion
EPD	Electron Photodetachment Dissociation
ESA	ElectroStatic Analyser
ESI	ElectroSpray Ionisation
ETD	Electron Transfer Dissociation
FC	Franck Condon
FCO	Frozen-Core Orbital
FOIS	First-Order Interacting Space
FRET	Förster Resonance Energy Transfer
FT-ICR	Fourier Transform Ion Cyclotron Resonance
FWHM	Full Width Half Maximum
G	Guanine
GFP	Green Fluorescent Protein
GGA	Generalised Gradient Approximation
GHO	Generalised Hybrid-Orbital
HBN	Hydrogen-Bonded Networks
HF	Hartree Fock
HOMO	Highest Occupied Molecular Orbital
IC	Internal Conversion
ICR	Ion Cyclotron Resonance
IE	Ionisation Energy
IMS	Ion Mobility Spectrometry
IR	InfraRed
IRMPD	InfraRed MultiPhoton Dissociation
ISC	InterSystem Crossing
IVR	Intramolecular Vibrational Redistribution
KER	Kinetic Energy Release
KID	keV Ion-induced Dissociation
LCAO	Linear Combination of Atomic Orbitals
LDA	Local Density Approximation
LIAD	Laser Induced Acoustic Desorption
LSCF	Local Self-Consistent Field
LUMO	Lowest Unoccupied Molecular Orbital
MALDI	Matrix Assisted Laser Desorption Ionisation
MBPT	Many-Body Perturbation Theory
MCP	MicroChannel Plate
MD	Molecular Dynamics
MECI	Minimum-Energy Conical Intersections
MeCN	Acetonitrile
MeOH	Methanol
MIKE	Mass-analysed Ion Kinetic Energy
MM	Molecular Mechanics
MO	Molecular Orbital

MR	Multi-Reference
MP	Møller Plesset (perturbation theory)
MS	Mass Spectrometry
Nd:YAG	Neodymium-doped Yttrium Aluminium Garnet
NEXAMS	Near Edge X-ray Absorption Mass Spectrometry
NIM	Normal Incidence Monochromator
NMR	Nuclear Magnetic Resonance
OPO	Optical Parametric Oscillator
PA	Proton Affinity
PAAA	Protonated Aromatic Amino Acid
PD	PhotoDetachment
PES	PhotoElectron Spectroscopy
	Potential Energy Surface
PGM	Plane Grating Monochromator
PID	Photo-Induced Dissociation
PMT	PhotoMultiplier Tube
PP	ProtoPorphyrin IX
PSD	Position Sensitive Detector
	Post Source Decay
PT	Proton Transfer
	Perturbation Theory
PYP	Photoactive Yellow Protein
QCP	Quantum-Capping Potential
QET	Quasi-Equilibrium Theory
QM	Quantum Mechanical
RCB	Repulsive Coulomb Barrier
RET	Resonance Energy Transfer
RF	RadioFrequency
Rh	Rhodopsin
RNA	RiboNucleic Acid
RRKM	Rice Ramsperger Kassel Marcus (rate constant expression)
R-TOF	Reflectron Time Of Flight
S	Singlet state
SDS	Sodium Dodecyl Sulfate
SED	Secondary Emission Detector
SF	Statistical Fragmentation
SID	Surface Induced Dissociation
SOMO	Single Occupied Molecular Orbital
SORCI	Spectroscopy-Oriented Conical Intersection
T	Thymine
	Triplet state
	Tryptophan
TCNQ	TetraCyaNoQuinodimethane
TD-DFT	Time-Dependent Density Functional Theory
TOF	Time Of Flight

U	Uracil
UV	UltraViolet
VAD	Vibrational AutoDetachment
VC	Vibrational Cooling
VDE	Vertical Detachment Energy
VFRAD	Vibrational Feshbach Resonance AutoDetachment
Vis	Visible
VUV	Vacuum UltraViolet
XC	eXchange Correlation

Contents

General Concepts

1

Steen Brøndsted Nielsen and Jean Ann Wyer

1.1 Electrostatic and Magnetic Fields

An ion with mass m, charge q and velocity v that encounters an electromagnetic field, composed of an electric field $\boldsymbol{E}$ and/or a magnetic field $\boldsymbol{B}$, will experience the Lorentz force $\boldsymbol{F} = q(\boldsymbol{E} + \boldsymbol{v} \times \boldsymbol{B})$. For both electrostatic parallel plate and cylindrical deflectors the potential difference V required to redirect an ion is dependent on the kinetic energy to charge ratio of the ion (Figs. 1.1 and 1.2). On the other hand, the magnitude of a magnetic field needed to deflect an ion along a radius of curvature r depends on the momentum to charge ratio of the ion (Fig. 1.3).

As the centripetal force is perpendicular to the direction of motion, the speed remains constant. Since the particle takes a circular path within the cylindrical deflectors, the angle of deflection is simply the angle, θ, subtended by the deflectors.

As the force on a moving charge due to the magnetic field is perpendicular to the velocity, the ion will take a circular path with no change in its kinetic energy.

1.2 Nucleic Acid Building Blocks

Nucleic acids are composed of nucleotides. Each building block contains a furanose sugar, a phosphate group and a base (Fig. 1.4). In DNA the sugar is deoxyribose while in RNA it is ribose, and the bond that links the sugar and the base together is called the glycosidic bond. The DNA bases are adenine (A), guanine (G), thymine (T), and cytosine (C), and the RNA bases are adenine, guanine, cytosine and uracil (U) (Fig. 1.5). An example of a DNA homopolymer of adenine (oligonucleotide) is shown in Fig. 1.6. The DNA double helix is formed when two complementary strands come together according to the specific binding of A with T and G with C (Watson-Crick base pairs, Fig. 1.5). Guanine-rich DNA strands can form G-quadruplex

S.B. Nielsen (✉) • J.A. Wyer
Department of Physics and Astronomy, Aarhus University, Aarhus C 8000, Denmark
e-mail: sbn@phys.au.dk; jeanwyer@phys.au.dk

S. Brøndsted Nielsen and J.A. Wyer (eds.), *Photophysics of Ionic Biochromophores*,
Physical Chemistry in Action, DOI 10.1007/978-3-642-40190-9_1,
© Springer-Verlag Berlin Heidelberg 2013

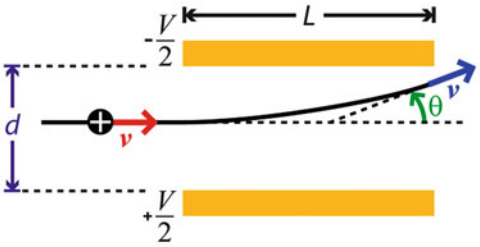

Fig. 1.1 Deflection of an ion using parallel plates: $V = \frac{E_{kin}}{q} \frac{2\, d \tan\theta}{L}$

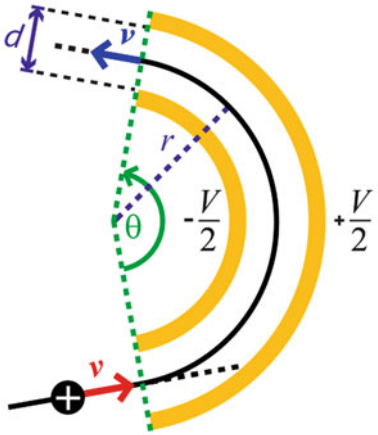

Fig. 1.2 Deflection of an ion using concentric cylindrical plates: $V = \frac{E_{kin}}{q} \frac{2\, d}{r}$

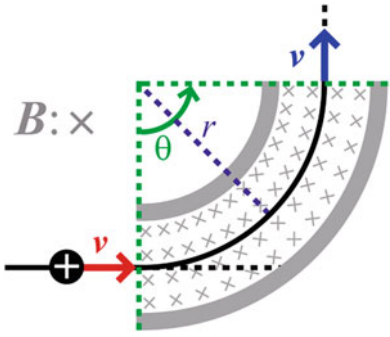

Fig. 1.3 Deflection of an ion using a magnetic field: $B = \frac{m\, v}{q} \frac{1}{r}$

structures, either by intra- or inter-molecular complexation. These complexes are built from stacked G-quartets comprised of four guanines that are hydrogen bonded in a planar motif around a central metal atom (Fig. 1.7).

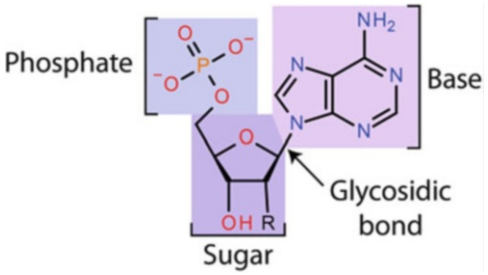

Fig. 1.4 Mononucleotide where the base is adenine. For DNA *R* represents H, while for RNA it represents OH

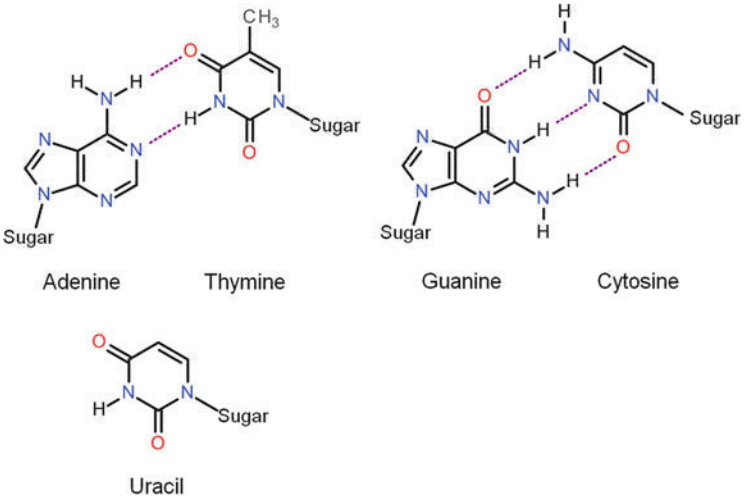

Fig. 1.5 Nucleobases. In DNA duplexes, A pairs with T and G with C

The phosphate group is negatively charged, which implies that nucleic acids are multiply charged anions in aqueous solution at neutral pH. Therefore duplex formation requires high salt concentrations to diminish the Coulomb repulsion between the strands. At low pH, both the phosphates and the bases are protonated, which results in positively charged species. Nucleic acids can therefore be produced in the gas phase both as anions and cations dependent on their protonation state.

1.3 Photoactive Amino acids and Peptides, and Their Structures

Aromatic amino acids strongly absorb light in the UV region and are therefore of particular relevance for this volume. They are phenylalanine, tyrosine, and tryptophan (Fig. 1.8). The π-conjugated network of the rings results in highly delocalised

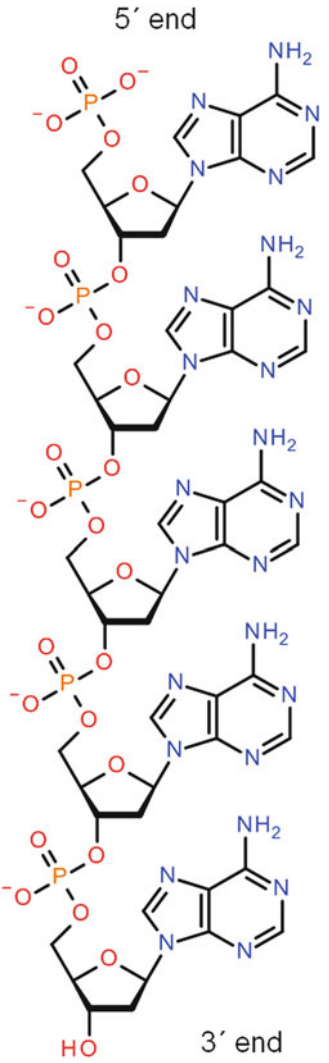

Fig. 1.6 A DNA homopolymer of adenine

molecular orbitals, and these amino acids thus absorb to the red of the other seventeen naturally occurring ones. Excitations in this region are typically $\pi\pi^*$ transitions. Due to these properties, peptides subjected to UV spectroscopic experiments often contain at least one aromatic amino acid.

A dipeptide is made when two amino acids join together, release a water molecule and form an amide bond (see Fig. 1.9). Addition of more amino acids in a similar way results in longer peptides. Proteins are peptides with a biological function, *e.g.*, transport of small molecules or enzymatic activity. A classification of the structural hierarchy was introduced by Linderstrøm-Lang. The sequence of amino acid residues is denoted the primary structure, while the secondary structure

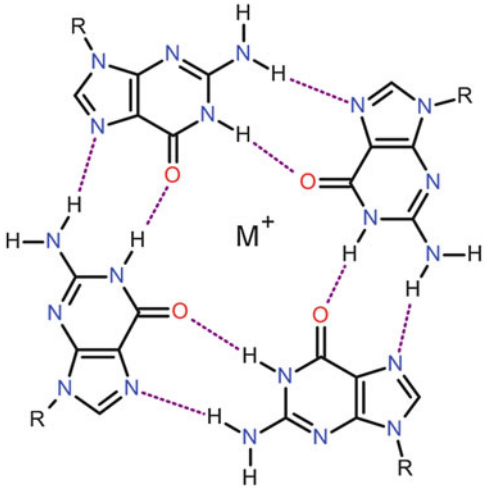

Fig. 1.7 Structure of a G-quartet

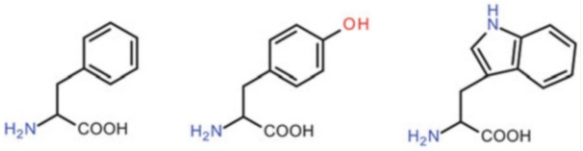

Fig. 1.8 Structures of phenylalanine (Phe, F), tyrosine (Tyr, Y), and tryptophan (Trp, W)

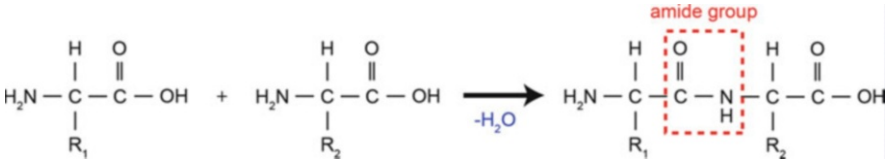

Fig. 1.9 Peptide formation from two amino acids. R_1 and R_2 represent the amino-acid side-chains

refers to the different folding motifs of the substructures, *e.g.*, α-helix, β-sheet, and random coil. How the substructures are organised relative to each other in three dimensions is called the tertiary structure. If a protein has more than one polypeptide chain, then the quaternary structure is the arrangement of the polypeptides relative to each other.

In gas phase, peptide basic groups, *e.g.* amino and guanidine groups, are easily protonated forming positively charged cations, while negatively charged anions are formed by deprotonation of carboxylic acid groups. In mass spectrometry the sequence of a peptide is determined by fragmentation, induced by either collisions after acceleration, electron capture, or photoexcitation, followed by mass spectrometric analysis of the fragment ions. The nomenclature for fragment ions is illustrated for a tetrapeptide in Fig. 1.10.

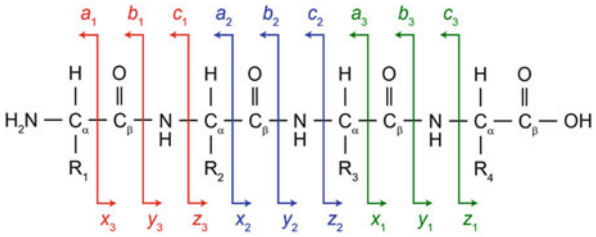

Fig. 1.10 In the Roepstorff, Fohlman and Biemann fragmentation nomenclature a fragment is labelled according to which bond in the repeating backbone series was broken, and whether it is the amino-terminal (N-terminal) or carboxyl-terminal (C-terminal) part. Cleavage of the C_α–C_β, C_β–N (amide or peptide bond), or N–C_α bonds result in *a*, *b*, or *c* fragments, and *x*, *y*, or *z* fragments for the N-terminal and C-terminal sections, respectively. The *subscript* refers to the number of amino-acid side-chains present

1.4 Photophysical Processes

A Jabłoński diagram (Fig. 1.11) is often used to illustrate photophysical processes, with the transitions between the different electronic states and their vibrational levels indicated. Absorption (A) of a photon induces a transition from the initial electronic state (S_0) to a higher-energy one (S_N), while when a photon is emitted the transition is to a lower state. Such a transition is called fluorescence (F) if there is no change in spin and for phosphorescence (P) if there is a change in spin. Internal conversion (IC) is a radiationless deexcitation process, whereby a molecule relaxes to a lower electronic state with the same spin. IC is faster between S_N and $S_{N\text{-}1}$ than $S_{N\text{-}1}$ and $S_{N\text{-}2}$ since the separation of the levels decreases with increasing *N*, and thus the nuclear wavefunctions overlap better. This implies that S_1 is populated quickly, and that the IC from S_1 to S_0 is the slowest. Hence most photochemistry occurs from S_1, and emission also normally occurs from there (Kasha's rule). While the energy may initially be localised in one specific vibrational mode, it is redistributed among all modes through a process known as intramolecular vibrational energy redistribution (IVR) that often occurs on sub-ps to ps timescales. (Notice, IC is sometimes also used to denote a transition between different vibrational levels.) In a solution, this excess vibrational energy dissipates to the solvent (*i.e.*, vibrational cooling) on a time scale that depends on the coupling strength between the solute and the solvent molecules. Intersystem crossing (ISC) is a radiationless transition to a state with a different spin. This is possible due to spin–orbit coupling and is particularly important if the S_1 lifetime is long. ISC back to the ground state also requires a spin flip, and as the overlap of the nuclear wavefunctions for T_1 and S_0 is low, it is an even slower process (Fig. 1.12).

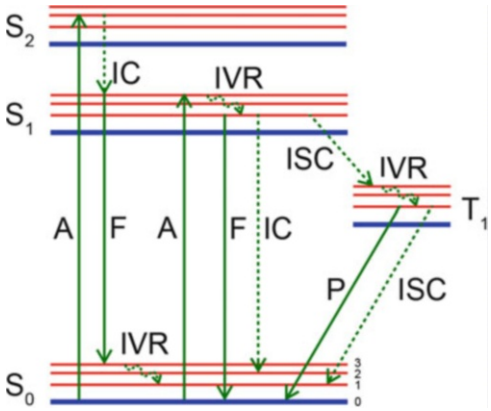

Fig. 1.11 A Jabłoński diagram indicating the electronic ground state (S_0), the first (S_1) and second (S_2) excited singlet states and the first triplet state (T_1). According to Hund's rule, T_1 is lower in energy than S_1. A number of vibrational energy levels are shown for each electronic state; the separation between vibrational levels decreases due to anharmonicity of the potential energy curve. Radiative transitions are depicted with *straight lines*, radiationless transitions with *dashed lines*, and the direction of the transition with an *arrow*. The difference in energy between the absorbed and emitted photons is called the Stokes shift

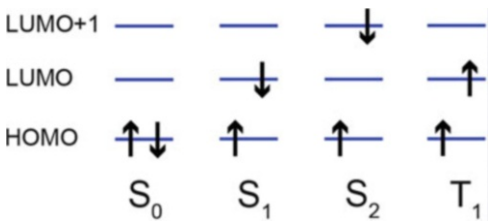

Fig. 1.12 Electronic configurations specified by occupation of orbitals and spin symmetry (each electron "*arrow*" is associated with a one-electron wavefunction): *HOMO* Highest Occupied Molecular Orbital; *LUMO* Lowest Unoccupied Molecular Orbital. The spin multiplicity of a molecule is $2S+1$, where S is the total spin quantum number. Singlet (S), doublet (D), and triplet (T) states are states with spin 0, ½, and 1, respectively

1.5 σ, π and n Orbitals, and Electronic Transitions

The combination of two atomic s orbitals results in two new molecular orbitals (MOs) that are denoted σ orbitals as when viewed from the side along the atom–atom axis they look like s orbitals (rotational symmetry). This is illustrated for the molecular hydrogen molecule in Fig. 1.13a. Due to the overlap of the atomic orbitals, the energy is different for the plus and minus combinations. The plus combination results in the bonding orbital labelled σ, while the minus combination gives the antibonding orbital labelled σ* (one nodal plane between the two nuclei). The σ orbital is lower in energy than the original s orbitals while the σ* orbital is

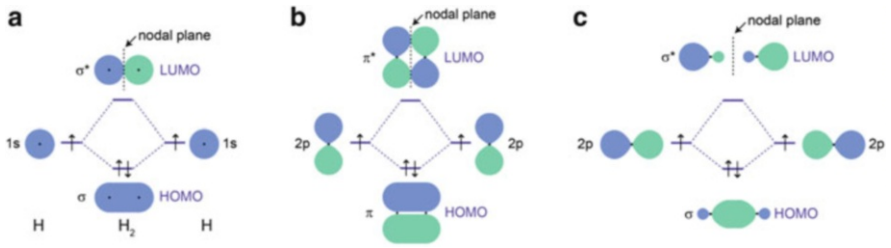

Fig. 1.13 Formation of molecular orbitals from atomic orbitals

higher in energy by more than the σ orbital is lowered. Popularly speaking, "the σ* orbital is more antibonding than the σ is bonding". (This follows from the variational principle and a non-zero orbital overlap integral. Notice that the energy of the H 1s orbital on the figure is not that of an isolated H atom (−13.6 eV) but has been lowered by the favourable interaction between the electron and the other nucleus at the distance where the bond is formed.). In a similar way, the linear combination of N p orbitals leads to N π orbitals; viewed from the side along the axis of the two atoms the two orbitals look like p orbitals, hence the name π orbitals. The simplest case for $N = 2$ is shown in Fig. 1.13b. The more p orbitals that overlap, the more delocalised the state is, and as a result the electronic transition redshifts (Fig. 1.14). It should also be noted that two p orbitals can combine to form σ orbitals (Fig. 1.13c). Atomic orbitals that do not participate in bonding are denoted non-bonding orbitals (n-orbitals) or lone-pair orbitals. As an example see the illustration of the water molecule in Fig. 1.15. All orbitals in a molecule are filled up according to the Aufbau principle (electrons fill the lowest-energy available orbitals first) and Pauli principle (no two electrons can have identical quantum numbers).

A transition from a σ orbital to a σ* orbital, *i.e.*, σσ* transition, is electronically allowed as the orbitals have different parity. Since the overlap of the two orbitals is large, the oscillator strength is high. Likewise for ππ* transitions. A charge-transfer transition from say a π orbital of an aromatic ring system to a σ* orbital of an ammonium group has a low oscillator strength due to the low orbital overlap. πσ* states can, however, be populated from long-lived photoactive ππ* states by internal conversion. The "allowed-ness" of an electronic transition also depends on whether spin is conserved or not and on the overlap of the nuclear wavefunctions between the two states.

Polar solvents induce shifts in absorption/fluorescence bands relative to those in vacuum. This is because solvent molecules stay still during light-induced electronic transitions, and while they are oriented in the optimal position for a favourable interaction with the initial state orbitals, they may not be in the prime position for the final state orbitals (Figs. 1.16 and 1.17a). A solvent therefore induces a blueshift in absorption for nπ* transitions (strong solvent dependence) (Fig. 1.17a). In contrast a redshift in absorption is often seen for ππ* transitions (Fig. 1.17b) where the dependence on solvent geometry is weak; instead the higher

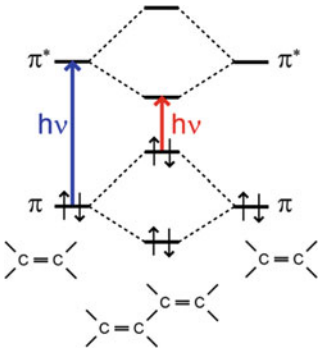

Fig. 1.14 Increased π conjugation causes the absorption to red shift

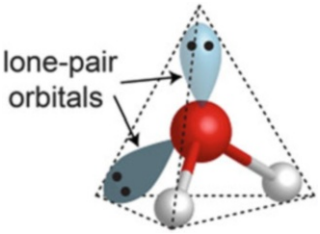

Fig. 1.15 A water molecule has a tetrahedral shape, with lone-pair orbitals occupying two of the vertices

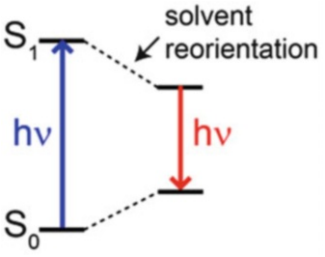

Fig. 1.16 Stokes shift is the difference between the positions of the absorption and emission band maxima

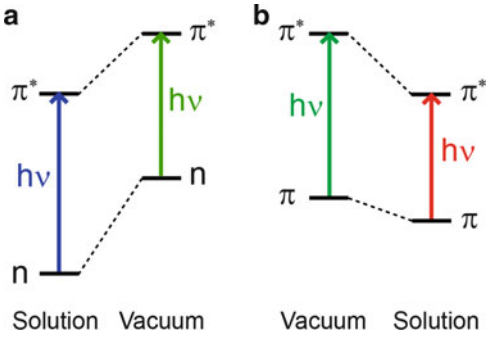

Fig. 1.17 (**a**) A polar solvent induces a blueshift for nπ* transitions. (**b**) A solvent induces a redshift for ππ* transitions

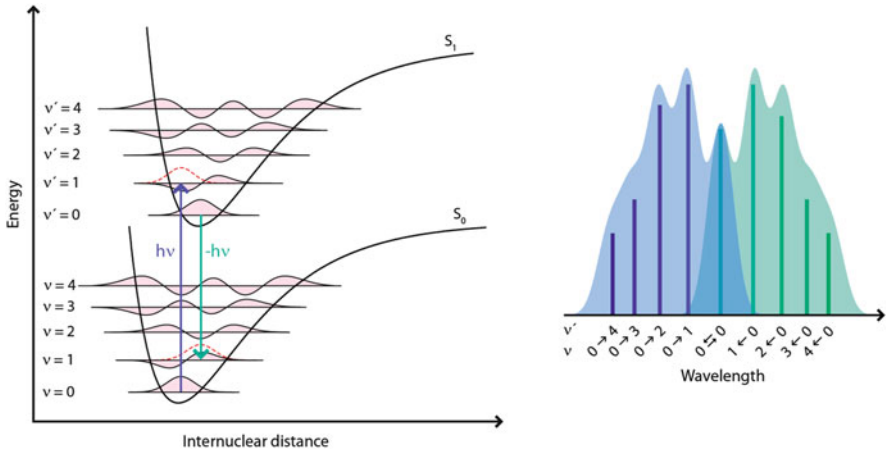

Fig. 1.18 *Left*: Illustration of the Franck-Condon principle for the electronic excitation/deexcitation of a diatomic molecule. Vertical transitions have the highest probability as they are associated with large overlap of the nuclear wavefunctions. The wavefunctions include one extra nodal point for each step up in quantum number v, and become increasingly concentrated at the turning points. The strongest transition will be to the vibrational level whose wavefunction has the largest overlap with the original wavefunction. Red dotted lines are drawn to indicate the initial nuclear wavefunctions. *Right*: The overall shape of the absorption band is determined by the overlap with each vibrational mode. As fluorescence is likely to occur from $v' = 0$ and the structures of S_0 and S_1 are similar, the emission band is often a mirror image of the absorption band (mirror-image rule)

polarisability of the excited state than that of the ground state increases the interaction energy between the chromophore and the solvent molecules.

1.6 The Franck-Condon Principle

According to the Born-Oppenheimer approximation, as nuclei move slowly compared to the far lighter electrons, electrons follow the nuclei instantaneously. Conversely, the nuclei adjust slowly to a change in the electronic state. This implies that in an electronic excitation the wavefunction for the nuclear motion is nearly the same immediately after as before the excitation (Fig. 1.18). The absorption spectrum of the molecule directly reflects this as the pattern is determined by the so-called Franck-Condon (FC) factors. For one particular vibrational level in the electronic excited state, this factor is calculated as the square of the overlap integral of the nuclear wavefunctions in the electronic ground and excited states. In other words, the FC factor is a measure of the relative importance of one vibrational component of an absorption band. The overall intensity of the electronic transition is obtained from the area under the absorption spectrum since the sum of all FC factors adds up to one.